Generation of user defined turbulent inflow conditions by an active grid for validation experiments

Kröger, Lars; Frederik, Joeri; Van Wingerden, Jan Willem; Peinke, Joachim; Hölling, Michael

DOI
10.1088/1742-6596/1037/5/052002

Publication date
2018

Document Version
Final published version

Published in
Journal of Physics: Conference Series

Journal of Physics: Conference Series

PAPER • **OPEN ACCESS**

Generation of user defined turbulent inflow conditions by an active grid for validation experiments

To cite this article: Lars Kröger *et al* 2018 *J. Phys.: Conf. Ser.* **1037** 052002

IOP Conf. Series: Journal of Physics: Conf. Series **1037** (2018) 052002 doi:10.1088/1742-6596/1037/5/052002

Generation of user defined turbulent inflow conditions by an active grid for validation experiments

Lars Kröger[a], Joeri Frederik[b],Jan-Willem van Wingerden[b], Joachim Peinke[a] and Michael Hölling[a]

[a] ForWind and Institute of Physics, University of Oldenburg, 26129 Oldenburg, Germany
[b] Delft Center for Systems and Control, Faculty of Mechanical, Maritime and Materials Engineering, Delft University of Technology, 2628 CD Delft, the Netherlands

E-mail: `lars.kroeger@uol.de`

Abstract. A wind tunnel experiment is presented which combines the use of controlled turbulent inflow conditions and a two-bladed model wind turbine utilizing a new control strategy called subspace predictive repetitive control (SPRC). The validation of the performance of SPRC was made under turbulent inflow conditions generated by an active grid. The $3m \times 3m$ active grid is used in this experiment using a unique method to generate reproducible atmospheric-like turbulent wind fields to act on a medium sized model wind turbine. This contribution is focussing on the detailed description of the experiment and its components and the analysis of the turbulent inflow by means of one and two point statistics. Exemplarily the impact of the new control strategy to the generated turbulent test cases are discussed.

1. Introduction

Because of the increasing energy consumption and the expansion of renewable energy the demands on wind energy converters are constantly increasing. Especially the development of new offshore wind turbines with higher energy production are of very high importance. As part of the Innwind.eu project, which had the overall objectives of the high performance innovative design of a beyond-state-of-the-art 10-20 MW offshore wind turbine and hardware demonstrators of some of the critical components, new mechanisms for active and passive rotor load control were developed. As the wind fields of the atmospheric boundary layer (ABL) acting on the rotor and the turbine are turbulent as shown in [1], the validation of these new concepts have to take place under controlled turbulent conditions. We present a wind tunnel experiment, which combines a model wind turbine equipped with these new control designs and a turbulent inflow generated by an so called active grid. The active grid is an instrument allowing us to generate turbulence with a wide range of different behaviour, additionally such turbulent flows can be repeated quite accurately. So it is possible to validate these new concepts using different turbulent inflow conditions.

2. Experiment

In this section a detailed description of the conducted experiment is given. Beginning with the new WindLab wind tunnel of the University of Oldenburg and its key component the active

IOP Conf. Series: Journal of Physics: Conf. Series **1037** (2018) 052002 doi:10.1088/1742-6596/1037/5/052002

grid. Followed by a brief description of the investigated model wind turbine of the Technical University of Delft. Concluding with the overall setup and measurement system.

Wind Tunnel
The experiment is conducted in a wind tunnel of the University of Oldenburg. It is a closed loop wind tunnel ('Göttinger' design type) and has a cross section of 3 x 3 m and a test section length of 30 m, which can be used in a closed or open test section configuration. Five optional test section segments of the dimension of $3 \times 3 \times 6m^3$ can be installed behind the contraction for the operation in closed configuration. A sketch of the wind tunnel can be seen in figure 1. The contraction of the nozzle has a ratio of 1:4, decreasing the outlet from 6 m $\times$ 6 m to 3 m $\times$ 3 m. Using four fans with a power of 110 kW each, thus resulting in 440 kW of electric power in total, wind speeds up to 42 m/s can be achieved when used with a closed test section. The maximum wind speed with an open test section is 32 m/s. Honey combs and fine meshes in front of the nozzle are reducing the turbulence intensity of the wind tunnel without any test subjects and in closed test section configuration to a maximum of 0.3 %. Prantl tubes before and after contraction are used for a closed loop wind speed control with an accuracy of $\pm$ 0.1 m/s for wind speeds higher than 3 m/s. Additionally a cooling system is installed to ensure constant temperature when measuring at higher wind speeds. The used cooling system has 192 kW of electric power resulting in 406 kW of effective cooling power.

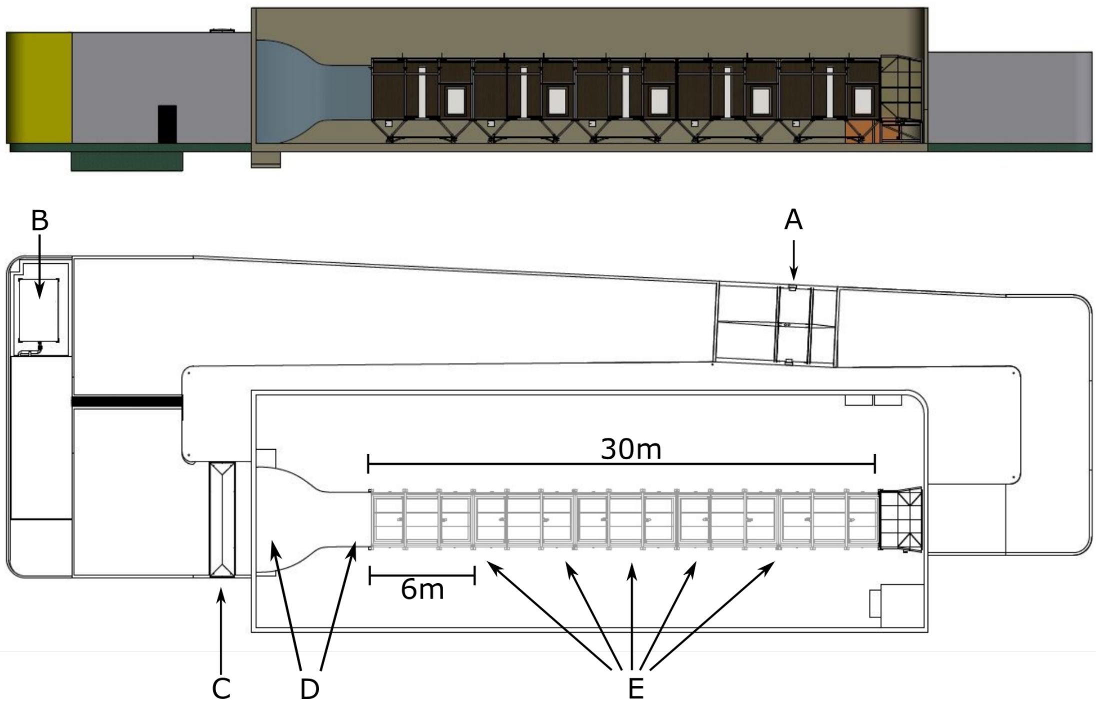

Figure 1. Schematic of the WindLab wind tunnel of the University of Oldenburg (above: side view; below: top view).
A: array of fans (4 $\times$ 110 kW); B: cooling system (406 kW of cooling power); C: honey combs and nets; D: prantl tubes; E: optional closed test section segments

Active Grid
The inflow of the wind tunnel gets modulated by an active grid, which is mounted to the wind tunnel outlet. A picture can seen in figure 2. The active grid as introduced by Makita [2] can be used to generate customized turbulence for wind tunnel applications. A nice overview of the work in active grid research was currently published in [3] The used active grid is dividing the cross section by 80 horizontal and vertical axes, every axes is 1.5 m long and covering half the distance from one side of the nozzle to the other, thus resulting in a mesh width of about 0.14 m. All of these axes are connected to servo motors in a manner that each can be controlled individually by a real time system. The servo motors are Kollmorgen VLM22C-DLNC-00 in combination with Kollmorgen servo drives (AKD-P00306-NBEC-0000) acting as power supply and monitoring device of the feedback. The motors are controlled via EtherCAT communication using a National Instruments Real Time Embedded Controller (NI PXIe-8135) and LabView Software. Square flaps are mounted to the axes, which are, depending on the orientation to the inflow, blocking and deflecting the wind. A close up picture of the flaps attached to the axes is shown in figure 3. The range of the cross section blockage possible in this setup is between a minimum of 21 % to a maximum of 92 %. Dynamic changes over time of the angle α of the flaps in respect to the inflowing wind are in the following described as excitation protocol ($\alpha(t)$). Primarily the excitation protocol defines the dynamics of the generated turbulence.
The process to develop an excitation protocol with specified dynamics is varying strongly on the generated wind field you want to achieve and is still one of the main topics of active grid research in our work group. In this study the active grids excitation protocol was designed to reproduce a free field velocity time series measured by three combined LiDAR systems. The measurements in the ABL were done by three short range, continuous wave WindScanner LiDARs operating in synchronised staring mode measurement at 97.7 Hz. The measurements are representing the inflow of a wind turbine with a hub height of 90 m. In order to reproduce these wind speed fluctuations in the wind tunnel a so-called transfer function for the active grid was measured and evaluated. This transfer function relates simple active grid movements that result in different solidity of the grid changing the wind speed at a certain position in the wind tunnel. Based on this the measured LiDAR time series can be transferred into active grid movements generating a velocity time series in the wind tunnel, which is scaled to the dimensions of the experiment using Taylor's hypothesis. Further information on this process could be found in [5].

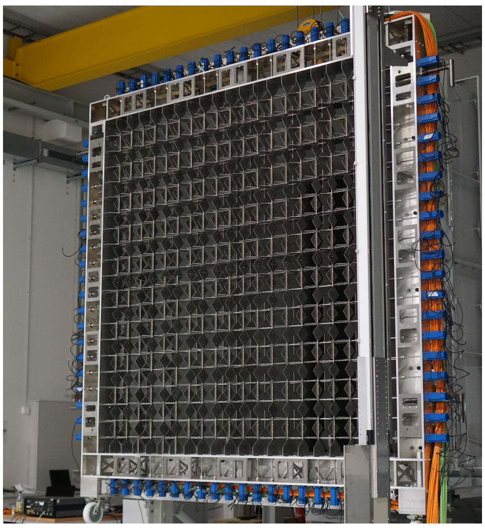

Figure 2. Active grid mounted to the wind tunnel nozzle.

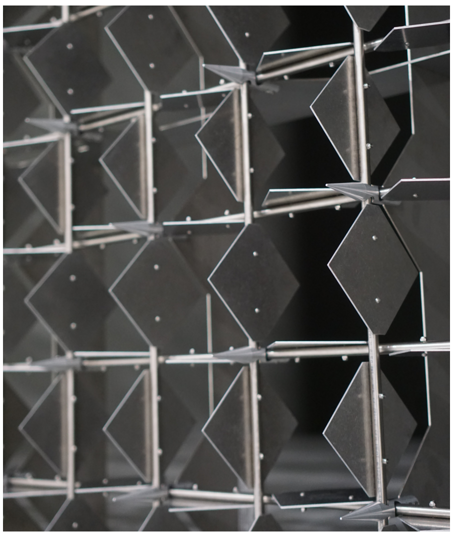

Figure 3. Close up of the active grid flaps, axes and intersections.

Model Wind Turbine

The model wind turbine of the TU Delft has a rotor diamenter of 1.6 m. The turbine is equipped with down scaled free-floating flap control and active pitch control. The model turbine is compared against the INWWIND.EU 10 MW reference turbine [8] in table 1. The scaling of the model wind turbine rotor is based on the ratio of the 1P frequency to the first blade flapwise frequency matching that of the 10 MW reference turbine. A further description of the model wind turbine can be found in [6]. A picture of the model turbine in front of the active grid is shown in figure 4. The specific details of the free-mounted flaps including the fabricating and results from the first tests in laminar inflow conditions can be found in [7]. The shaft is instrumented with a torque transducer and speed encoder, and is mechanically connected to the generator. The turbine is direct-drive; the rotor speed is the same as the generator speed. The generator is in turn connected electrically in series with an adjustable dump load amenable to resistance control. Thus, in principle this setup can also provide torque control. However, in this series of tests, the resistance of the dump load is kept constant. This implies that the wind turbine is in constant torque operation, and its rotor speed rises linearly with the incoming wind speed. This form of control deviates from classical variable-speed variable-pitch turbine control, which utilises collective pitch to ensure constant speed regulation above rated wind speed. However, the variable-speed constant load operation of the scaled turbine serves three purposes: over speed behaviour can be investigated, which may induce flutter, below-rated turbine behaviour can be emulated, and the use of adaptive control can be evaluated in terms of its ability to retune itself to adapt to changed operating conditions. The algorithm focused on in this contribution is the subspace predictive repetitive control [7] which is using the individual pitch control of the turbine.

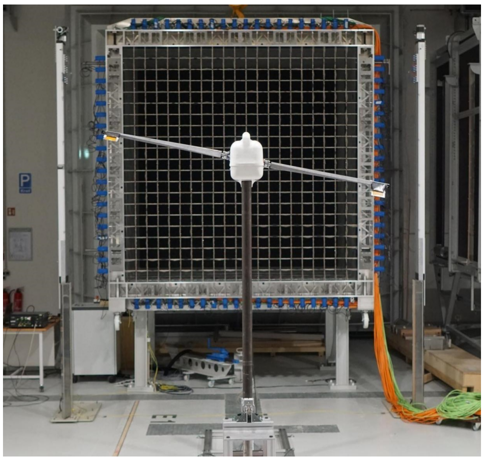

Figure 4. Model wind turbine in front of 3 m x 3 m active grid.

Experiment

The experiment was performed in two parts, the characterization of the turbulent inflow and the actual test with the model wind turbine. All of them in the open test section configuration of the wind tunnel. Four different turbulent test cases are generated by the active grid to act on the model wind turbine. Two of this test cases are used as references using the active grid in a static way keeping the axes steady at a certain position, therefore working like a regular grid. Acting as reference test case, with the lowest degree of turbulence, all of the axes are hold at the position of minimal blockage ($\alpha = 0°$; 21 %). As a test case with slightly increased turbulence intensity

Table 1. Parameter Comparison of the scaled turbine. [6]

	Reference turbine [8]	Scaled rotor
Rated wind speed (m/s)	11.4	6.5
Tip speed ratio (-)	7.86	3
Rated rotational speed (rpm)	9.6	230
Fore-aft tower mode (Hz)	0.25	20.73
Side-side tower mode (Hz)	0.25	20.73
First flapwise mode (Hz)	0.56	15
Ratio 1st blade freq. to 1P (-)	3.5	3.913

the blockage was increased to 43% ($\alpha = 45°$). In the other two test cases the grid is utilised in the active way using excitation protocols. The first one, later referred to as gusts protocol, is used to generate reoccurring but non-periodic gusts. The last turbulent test case was using a protocol based on LiDAR measurements done in the atmospheric boundary layer, with the goal to generate wind speed fluctuations along the main wind direction with comparable dynamics as the measured data but downscaled to the model wind turbine size and therefore referred to as LiDAR protocol. All the measurements were repeated for three different mean wind speeds (4 m/s, 4.5 m/s and 5 m/s). The turbulent inflow was measured by a Dantec Dynamics 2 D hot wire probe at the position of the model wind turbine for the validation measurements of the control algorithms. The acquired wind speed time series are sampled at 20 kHz with a 10 kHz low pass filter. Measurement positions are the hub of the model wind turbine (centerline) and shifted 1 m to either side of the model turbine to determine variations of the inflow over the diameter of the rotor. The location of the hot wire and turbine down stream of the active grid were at 3 m, thus 20 mesh sizes.

3. Results

In this section the results of the characterization of the turbulent inflow are shown and some exemplary results of the subspace predictive repetitive control (SPRC) algorithm reacting to the incoming turbulence.

Turbulent Inflow

One of the main differences of the four different turbulent cases is the turbulence intensity (TI). In table 2 the results of the four test cases at a mean wind speed of 5 m/s are shown for the measurement position at the centerline and for the shifted positions, corresponding to the rotor tip. Here and in the following analysis just the results for the highest mean wind speed of 5 m/s are shown as the differences in the characteristics are minor. For the static test cases the lower turbulence intensities are observed, by using excitation protocols the turbulence intensities can be increased. Because the wind tunnel is working in an open jet configuration the TI is increasing to the sides as the steady air is interacting with the air flow, as can be seen for the shifted measurement positions. One of the benefits of the active grid to regular grids can be seen in the relatively high turbulence intensity of 8.8% at a distance of 20 mesh sizes down stream of the grid, when used with an excitation protocol. For regular grids higher turbulence can just be achieved directly behind the grid as the decay of the turbulence is decreasing exponentially.

Furthermore the fluctuations of the wind speed time series are reproducible by repeating the active grid excitation $\alpha(t)$. In figure 5 three measured wind speed time series are shown

Table 2. Turbulence intensity at different measurement positions for the four test cases

Mode	**Centerline TI** [%]	**Shifted TI -1m** [%]	**Shifted TI +1m** [%]
Static 0°	2.5	2.7	2.7
Static 45°	3.7	5.0	5.2
Gusts	4.2	7.1	7.2
LiDAR	8.8	10.1	10.2

generated by the LiDAR excitation protocol. The 20 kHz data was filtered with a moving average over 1000 samples and all filtered time series match very well. For reference an unfiltered time series is added in light grey. Examination of the filtered data with normalized cross correlation shows a very good resemblance with correlation coefficient values better than 0.85, for the shifted positions the values decrease to 0.74. This reproducible behaviour of the wind speed time series can be validated also for the gusts protocol. Using the active grid in a static way the generated turbulence has a constant mean velocity and standard deviation of the wind speed fluctuation depending on the blockage of the active grid. Resulting in randomly distributed fluctuations in the flow which are not correlating to each other in a direct comparison of the time series if measurements are repeated. Nonetheless if the power spectra are used to get a better impression about the reproducibility of the four different turbulent test cases we can find a good agreement for the active as well as the static test cases. Every turbulent scenario was measured five times and the resulting power spectra smoothed by frequency bin averaging are shown in figure 7. Like in the direct comparison of the wind speed time series generated by the LiDAR excitation protocol the power spectra for all the different test cases are matching very well. Besides a significant increase of the lower frequencies when comparing the power spectra of the LiDAR and gusts excitation to the static reference cases can be observed, presumably the reason that higher turbulence intensities can be achieved. The amplified lower frequencies are in the range of 0.05 Hz to 10 Hz taking into account the mean wind speed of 5 m/s and the Taylor hypothesis this results in structures in the size of 0.5 m to 100 m or 0.5 to 60 rotor diameters. Looking at wind turbines in situ with a rotor radius of around 100 m and atmospheric turbulence with length scales in the order of kilometers this is depicting real operating conditions way better than the use of regular grids which generated length scales are in the order of the mesh sizes. The power spectra for the shifted positions are showing a supplementary increase of energy at the beneficial lower frequencies as the higher TI already suggested.

The intermittency of the generated flow fields is estimated using the shape parameter λ^2 according to

$$\lambda^2(\delta u) = \frac{1}{4}\ln\left(\frac{\langle(\delta u - \langle\delta u\rangle)^4\rangle}{3\sigma_{\delta u}^4}\right), \tag{1}$$

where δu is the velocity increment defined by

$$\delta u = u(t+\tau) - u(t), \tag{2}$$

and $\sigma_{\delta u}$ is the standard deviation of the increment time series and τ represents a time lag. The shape parameter is basically the normalized fourth moment of a given time series, a value of zero hereby represents a gaussian distributed probability density function values of non zero refer to time series with more extrem events and therefore intermittent behaviour of the time series. In figure 8 the shape parameter for all four test scenarios are shown in dependence of the time lag τ. The static test cases and the gusts protocol are slightly intermittent at the

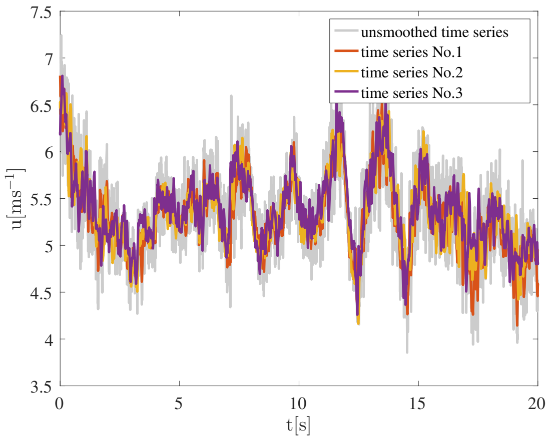

Figure 5. Wind speed time series behind the active grid using the LiDAR excitation protocol

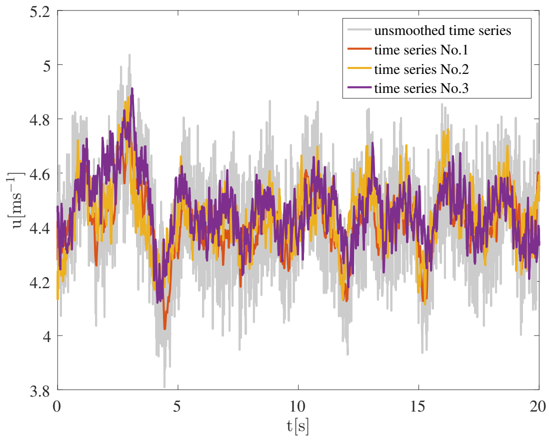

Figure 6. Wind speed time series behind the active grid using the gust excitation protocol

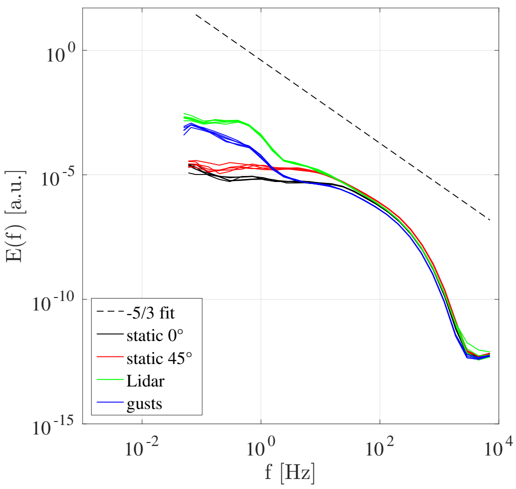

Figure 7. Power spectra of the four different test cases.

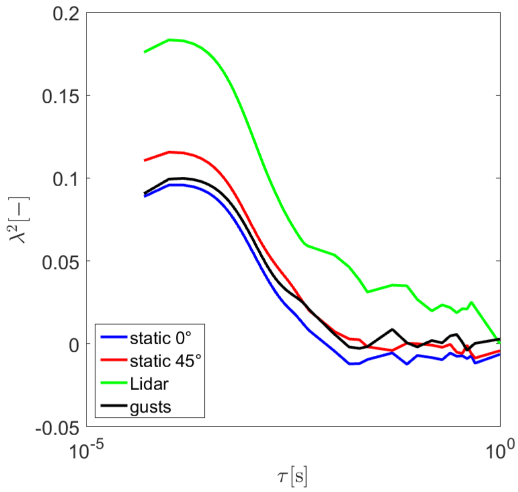

Figure 8. Shape parameter λ^2 of the four different test cases.

smallest scales and gaussian distributed on larger scales, just the LiDAR excitation is showing stronger intermittent behaviour for the smaller scales which is also decreasing to the larger time scales. As the turbulent fields acting on wind turbine are intermittent as shown in [1] the LiDAR excitation protocol is generating in this experiment a turbulent field which is the most realistic in comparison to atmospheric wind data.

Control Algorithm
Exemplary the influence of turbulence on the load measured on the wind turbine model is presented. Figure 9 shows the blade loads and blade root loads in the frequency domain (FD) for no control and SPRC in the turbulent LiDAR and the open grid reference inflow conditions for the wind speed of 5 m/s. When comparing the loads of model turbine without any control, the increased TI, when the LiDAR protocol is used, results in wider peaks of the blade root bending moments than in the static open grid reference case. Looking at the bending moments in FD the widening of the peaks is even more striking. The sharp peaks associated with the rotor

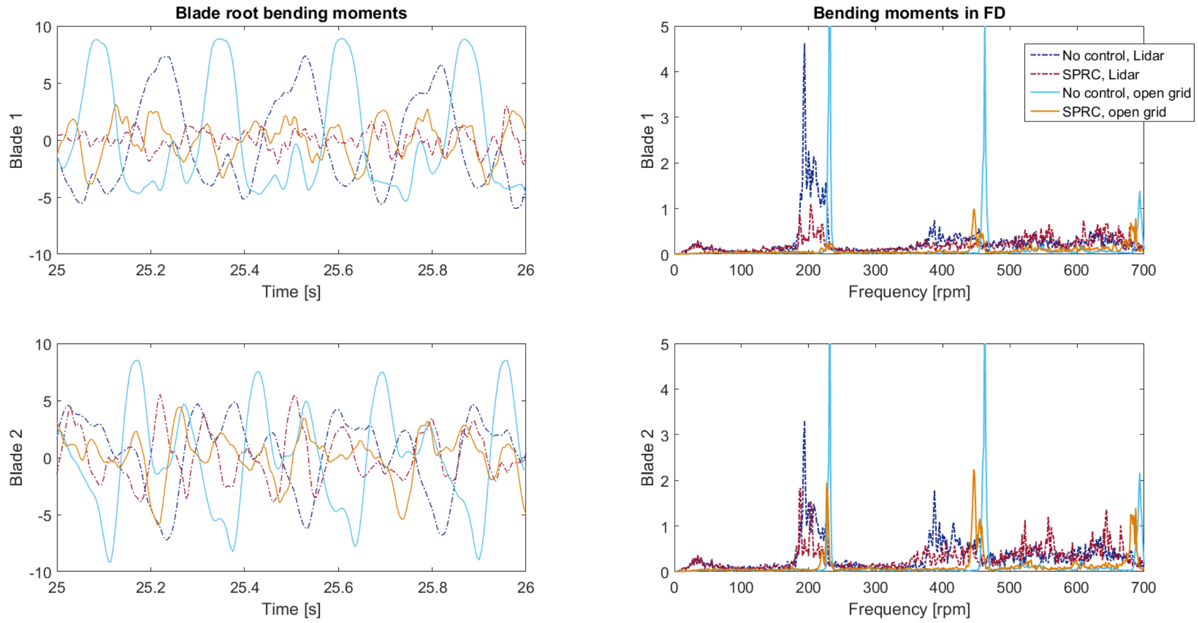

Figure 9. Blade loads and blade root loads in the frequency domain (FD) for no control and SPRC for laminar and turbulent inflow

speed in the static open grid reference cases are getting wider for the more turbulent LiDAR test case, this is due to higher wind speed fluctuations thus a varying of the rotor speed. Using the SPRC control algorithm a significant reduction of the 1P and 2P loads can be observed for both shown test cases. The use of a turbulent wind field based on atmospheric wind speed data validates the ability of the controller to react to changes in wind conditions. Differences in the strength of the bending moments peaks are due to imperfections of the turbine, which is not completely symmetrical. Moreover the used control algorithm (SPRC) determines the optimal control for each blade individually.

4. Conclusions

Four different turbulent inflow conditions could be generated and analyzed. The characteristics of the generated flow fields could be varied for several parameters as the turbulence intensity, the frequency range of the power spectra and intermittency. Additionally the reproducibility of a turbulent wind speed time series at a certain position in the wind tunnel could be demonstrated. The generated turbulent fields vary between a nearly laminar flow as reference and a more turbulent flow with intermittent behaviour and scaled frequency range of the power spectra to match the ratio of the rotor diameter of the model wind turbine to the conditions a real turbine faces in the atmosphere.
Thus a unique setup to test a model wind turbine and implemented control algorithms to reduce the acting loads under turbulent inflow conditions could be presented. A comparison with and without the new SPRC feedback control strategy could be made. By using turbulence with atmospheric like properties the applicability of the new control concepts to real wind turbines could be validated. As SPRC control is just using the individual pitch control mechanisms which is already standard in every industrial wind turbine this new control approach is applicable to a full scale turbine without major difficulties. Further information about the control algorithms

and a comparison to conventional individual pitch control can be found in [9] [10].

Acknowledgments
The measured LiDAR time series of wind data was provided by the WindScanner Research and Innovation team members Nikolas Angelou, Mikael Sjholm and Torben Mikkelsen at the DTU Ris campus as part of the Smart Blades project. The pre-processing of this data was done by Marijn van Dooren from ForWind. This work was supported by INNWIND.EU project supported by the Seventh Framework Programme (FP7) under Grant Agreement No. 308974 and by the Ministry for Science and Culture of Lower Saxony through the funding initiative Niedersächsisches Vorab (project ventus efficiens).

References
[1] Wächter M. et al. The turbulent nature of the atmospheric boundary layer and its impact on the wind energy conversion process,, Journal of Turbulence, 13, N26, 2012
[2] Makita, H., Realization of a large-scale turbulence field in a small wind tunnel, Fluid Dyn. Res. 8, 1991
[3] Mydlarski, L., A turbulent quarter century of active grids: from Makita (1991) to the present, Fluid Dyn. Res. 49, 2017
[4] Knebel et al., "Atmospheric wind field conditions generated by active grids", Exp Fluid 51, 2011
[5] Reinke, N., "Application, Generation and Analysis of Turbulent Flows", PhD Thesis University of Oldenburg, 2017.
[6] Navalkar et al., "Wind tunnel tests with combined pitch and free-floating flap control: data-driven iterative feedforward controller tuning", Wind Energ. Sci., 1, 2016
[7] Navalkar ST et al., "Subspace predictive repetitive control for variable pitch wind turbines.", IEEE Trans. Control Syst. Technol., 2015
[8] Bak C. et al, "Description of the DTU 10 MW reference wind turbine.", DTU Wind Energy, Roskilde, Denmark, Tech. Rep. I-0092, 2013
[9] Frederik J. A., Kröger L., Gülker G., Van Wingerden J. W. "Data-driven repetitive individual pitch control: wind tunnel experiments under turbulent wind conditions" Under review, 2018
[10] Frederik J. A., Kröger L., Peinke J., Hölling M. and van Wingerden J. W. "Validating subspace predictive repetitive control under turbulent wind conditions with wind tunnel experiment" Proc. Sci. of Making Torque from Wind. 2018